ACADEMIC
PRESS

The crystal structure, vibrational spectra, and thermal behavior of dilithium piperazinium(2+) selenate tetrahydrate and dilithium N,N'-dimethylpiperazinium(2+) selenate tetrahydrate

Jiří Plocek, David Havlíček,* Ivan Němec, Ivana Císařová, and Zdeněk Mička

Department of Inorganic Chemistry, Faculty of Science, Charles University of Prague, Albertov 2030, 128 40 Prague 2, Czech Republic

Abstract

The crystal structure of dilithium piperazinium(2+) selenate tetrahydrate has been solved; this substance crystallizes in the triclinic space group $P\bar{1}$, $a = 7.931(2)$ Å, $b = 7.974(2)$ Å, $c = 7.991(2)$ Å, $\alpha = 106.99(2)°$, $\beta = 101.83(2)°$, $\gamma = 119.28(2)°$ $Z = 1$, $R = 0.0280$ for 1489 observed reflections. A similar compound, dilithium N,N'-dimethylpiperazinium(2+) selenate tetrahydrate crystallizes in a monoclinic system with space group $P2_1/c$ and lattice parameters $a = 7.338(1)$ Å, $b = 8.792(2)$ Å, $c = 12.856(1)$ Å, $\beta = 92.04(2)°$, $Z = 2$, $R = 0.0334$ for 1462 observed reflections. Both structures are centrosymmetric with center of symmetry in the center of eight membered ring formed with two SeO_4 tetrahedra and two LiO_4 tetrahedra connected through tops. The two remaining oxygens on each Li atom come from water molecules. The FTIR and FT Raman spectra of both natural and N,O-deuterated substances have been measured and studied. The thermoanalytical properties were studied using TG, DTG and DTA methods in the temperature range 293–873 K for piperazinium derivative and in the range 293–523 K for dimethylpiperazinium derivative. DSC measurements were carried out in the temperature range 95–343 K. No phase transition was found in this temperature region for either of the compounds.

© 2002 Elsevier Science (USA). All rights reserved.

Keywords: Dilithium piperazinium(2+) selenate tetrahydrate; Dilithium N,N'-dimethylpiperazinium(2+) selenate tetrahydrate; Crystal structure; Vibrational spectra; Thermal behavior

1. Introduction

Alkali metal selenates double salts with piperazine and its derivatives have not been described in the literature yet. The solubility diagrams, crystal structures, thermal behavior and vibrational spectra of piperazinium(2+) selenate monohydrate and N,N'-dimethylpiperazinium(2+) selenate have been studied so far [1]. Of the relative compounds of sulfuric acid and piperazine, preparation of piperazinium(2+) sulfate monohydrate [2] and piperazinium(2+) hydrogen sulfate [3] have only been described. This paper deals with the preparation of dilithium piperazinium(2+) selenate tetrahydrate (Li$_2$pipz(SeO$_4$)$_2$·4H$_2$O) and dilithium N,N'-dimethylpiperazinium(2+) selenate tetrahydrate (Li$_2$Me$_2$pipz(SeO$_4$)$_2$·4H$_2$O) on the basis of study of

their solubility diagrams, crystal structures, vibrational spectra, and thermal behavior.

This work, which is part of our project of searching for a new potentially ferroelectric substances or fast proton conductors, is concerned with the study of the type of salts of inorganic acids with large organic bases. In these compounds, changes in the dynamic behavior of H-bonds protons can lead to the formation of phases with interesting physical properties [4].

2. Experimental

The solubility study was carried out using the Schreinemakers method [5]. Samples were tempered at 293 K and occasionally shaken. Establishment of equilibrium was controlled by measuring the refractive index and took about 30 days.

The X-ray data collections were carried out on an Enraf-Nonius CAD4-MACH III four-circle

*Corresponding author. Fax: +420-2-21952378.

E-mail address: havlicek@prfdec.natur.cuni.cz (D. Havlíček).

diffractometer (Mo$K\alpha$ radiation, graphite monochromator). The intensity was corrected for the Lorentz-polarization factor and absorption. In the case of $Li_2pipz(SeO_4)_2 \cdot 4H_2O$ absorption correction was performed by analytical method from crystal shape using JANA98 softare [6], while in the case of $Li_2Me_2pipz(SeO_4)_2 \cdot H_2O$ absorption correction was performed by empirical method using psi-scan (PLATON software [7]). The positions of the non-hydrogen atoms were determined using direct methods (SIR-92) [8], and the hydrogen atoms were localized on differential Fourier maps. The thermal parameters for the non-hydrogen atoms were refined anisotropically and, for the hydrogen atoms, isotropically. Refinement of the coordinates and the thermal parameters was carried out by the least-squares method using the SHELX 97 program [9]. The basic crystallographic data and the details of the measurement and refinement are summarized in Table 1. A list of the observed and calculated structural factors and the anisotropic displacement factors are available from the authors upon request.

The IR spectra of nujol and fluorolube mulls were recorded on a Mattson Genesis FTIR spectrometer (2 cm^{-1} resolution, Beer-Norton medium apodization) in the 400–4000 cm^{-1} region.

Raman spectra were recorded on a Bruker Equinox 55/S FTIR spectrometer with a FRA 106/S Raman module (2 cm^{-1} resolution, Blackman-Harris 4-Term apodization, 1064 nm NdYAG laser excitation, 300 mW power at the sample) in the 90–4000 cm^{-1} region.

DSC measurements were carried out on a Perkin-Elmer DSC 7 power-compensated apparatus in the 95–343 K°temperature region (helium atmosphere). A heating rate of 10 K/min was selected to measure approx. 10 mg of finely ground sample placed in an aluminum capsule.

Table 1
Basic crystallographic data, data collection and refinement parameters of $Li_2pipz(SeO_4)_2 \cdot 4H_2O$ and $Li_2Me_2pipz(SeO_4)_2 \cdot 4H_2O$

	$Li_2pipz(SeO_4)_2 \cdot 4H_2O$	$Li_2Me_2pipz(SeO_4)_2 \cdot 4H_2O$
Empirical formula	$C_4H_{20}Li_2N_2O_{12}Se_2$	$C_6H_{24}Li_2N_2O_{12}Se_2$
Formula weight	460.02	488.08
Temperature (K)	150(2)	150(2)
Wavelength (Å)	0.71069	0.71069
Crystal system, space group	Triclinic, $P\bar{1}$	Monoclinic, $P2_1/c$
Unit-cell dimensions	$a = 7.931(2)$ Å, $\alpha = 106.99(2)°$	$a = 7.338(1)$Å, $\alpha = 90°$
	$b = 7.974(2)$ Å, $\beta = 101.83(2)°$	$b = 8.792(2)$ Å, $\beta = 92.04(2)°$
	$c = 7.991(2)$ Å, $\gamma = 119.28(2)°$	$c = 12.856(1)$ Å, $\gamma = 90°$
Volume (Å^3)	383.14(17)	828.9(2)
Z, Calculated density (g/cm^3)	1, 1.994	2, 1.956
Absorption coefficien (mm^{-1})	4.23	4.521
$F(000)$	228	488
Crystal size (mm)	$0.8 \times 0.7 \times 0.6$	$0.4 \times 0.35 \times 0.3$
θ range for data collection (deg)	2.93–25.97	2.78—24.95
Index ranges	$h(-9;9)$, $k(-9;9)$, $l(0;9)$	$h(0;8)$, $k(0;15)$, $l(-15;15)$
Reflections collected/unique	1489/1489 [$R(int) = 0.0000$]	1575/1462 [$R(int) = 0.0169$]
Completeness to θ	100.0%, $\theta = 25.97$	100.0%, $\theta = 24.95$
Refinement method	Full-matrix least-squares on F^2	Full-matrix least-squares on F^2
Data/restraints/parameters	1489/0/141	1462/0/158
Goodness-of-fit on F^2	1.061	1.167
Final R indices [$I > 2\sigma(I)$]	$R_1 = 0.0280$, w$R_2 = 0.0719$	$R_1 = 0.0334$, w$R_2 = 0.0870$
R indices (all data)	$R_1 = 0.0289$, w$R_2 = 0.0726$	$R_1 = 0.0334$, w$R_2 = 0.0870$
Extinction coefficient	0.78(2)	0.038(3)
Largest diff. peak and hole (e/Å)	1.238 and –1.119	0.991 and –1.356
No. and θ range of reflections for unit-cell determination	25, 13°–15.5°	25, 13°–14.5°
Scan technique	θ–2θ	θ–2θ
No. of standard reflectoins	3	3
Standard reflections monitored in interval (min)	60	60
Intensity variation	2.5	1.4
Function minimized	$\left[\sum \left(w(F_o^2 - F_c^2) \right)^2 / \sum \left(w(F_o^2)^2 \right) \right]^{1/2}$	$\left[\sum \left(w(F_o^2 - F_c^2) \right)^2 / \sum \left(w(F_o^2)^2 \right) \right]^{1/2}$
Weighting scheme	$w = [\sigma^2(F_o^2) + 0.0572P^2 + 0.37P]^{-1}$ $P = [F_o^2 + 2F_c^2]/3$	$w = [\sigma^2(F_o^2) + 0.0675P^2 + 0.20P]^{-1}$ $P = [F_o^2 + 2F_c^2]/3$

Thermoanalytical properties were studied using TG, DTG, and DTA recordings. The measurements were carried out on a Derivatograph OD-102 instrument from MOM Budapest. A static atmosphere (air) was used in a 293–873 K temperature range for piperazinium(2+) derivative and in 293–523 K temperature range for dimethylpiperazinium derivative at a heat rate of 10 K/min.

Determination of Se(VI) [10] was carried out by potentiometric titration of Br_2, released by the reaction of sample with KBr in HCl medium, by hydrazinium(2+) sulfate. Lithium was determined by means of the AAS method using a Varian Techtron 1200 apparatus.

3. Results and discussion

3.1. Solubility study and salts preparation

The solubility diagram in the Li_2SeO_4–pipzSeO_4–H_2O system at 293 K is depicted in Fig. 1. In the figure, we can find the crystallization field of the initial $Li_2SeO_4 \cdot H_2O$ (field 2), the crystallization field of dilithium piperazinium(2+) selenate tetrahydrate (field 4) and crystallization field of piperazinium(2+) selenate monohydrate (field 6). Fields 3 and 5 correspond to equilibrium between two solid phases and a solution with compositions corresponding to eutonic points C and D respectively. Point C corresponds to a composition of

33.57% Li_2SeO_4, 17.97% pipzSeO_4, and 48.46% H_2O, and point D corresponds to a composition of 13.98% Li_2SeO_4, 42.65% pipzSeO_4, and 43.46% H_2O. Dilithium piperazinium(2+) selenate tetrahydrate is congruently

Table 2
Fractional atomic coordinates (for non-H atoms $\times 10^4$, for H atoms $\times 10^3$) and equivalent or isotropic displacement factors of $Li_2pipz(SeO_4)_2 \cdot 4H_2O$ $U_{eq} = 1/3 \sum_i \sum_j U_{ij}\mathbf{a}_i^* \mathbf{a}_j^* \mathbf{a}_i\mathbf{a}_j$

|	x	y	z	$U_{(eq)}$
Se(1)	5923(1)	−1988(1)	2823(1)	10(1)
O(1)	7250(3)	620(3)	3566(3)	20(1)
O(2)	5787(3)	−2572(4)	4612(3)	23(1)
O(3)	7179(3)	−2791(3)	1830(3)	16(1)
O(4)	3511(3)	−3233(3)	1220(3)	16(1)
O(5)	−468(4)	−6268(4)	−2648(3)	20(1)
O(6)	3830(4)	−3220(4)	−2822(4)	22(1)
C(1)	11107(5)	−980(5)	100(4)	17(1)
C(3)	10779(5)	1915(5)	1705(4)	16(1)
N(2)	10925(4)	160(4)	1818(4)	15(1)
Li	2575(7)	−4857(8)	−1544(7)	16(1)
H(11)	1120(6)	−202(6)	24(5)	14(8)
H(12)	1253(7)	12(7)	13(6)	30(10)
H(21)	974(6)	−76(6)	187(5)	18(9)
H(22)	1184(7)	65(6)	271(6)	19(10)
H(31)	1194(6)	284(6)	166(5)	10(8)
H(32)	1062(6)	260(6)	283(5)	25(10)
H(51)	−125(9)	−635(8)	−234(7)	40(15)
H(52)	−107(6)	−714(6)	−375(6)	16(9)
H(61)	357(7)	−242(8)	−301(6)	33(11)
H(62)	403(9)	−350(9)	−343(8)	35(17)
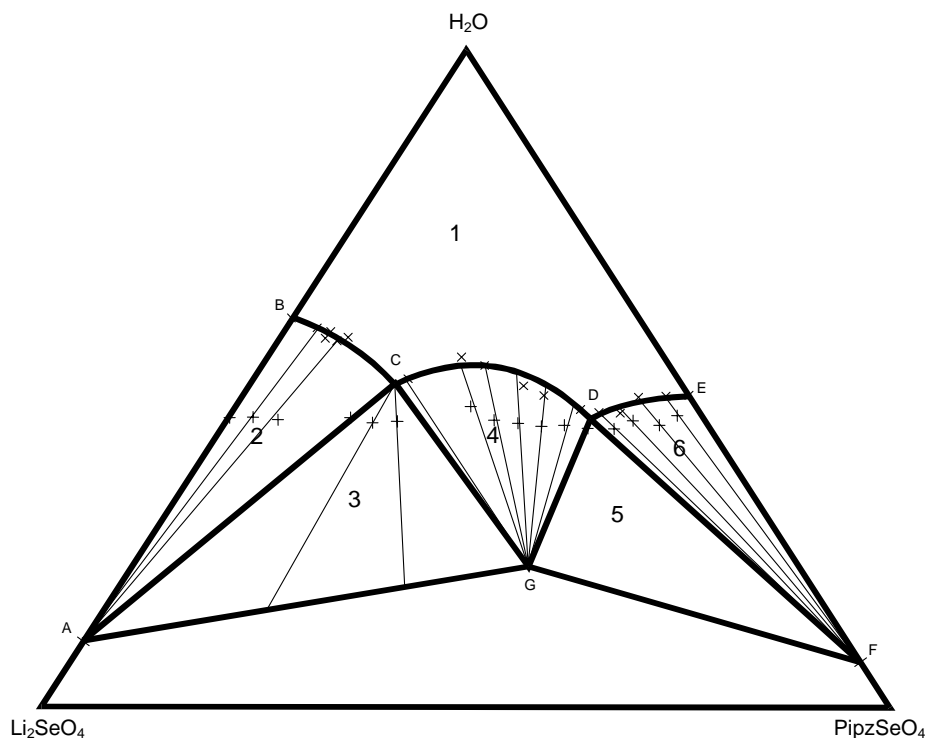
Fig. 1. Solubility diagram in the Li_2SeO_4–pipzSeO_4–H_2O system at 293 K.

soluble. Therefore, this substance was prepared by dissolving a mixture (in molar ratio 1:1) of $Li_2SeO_4 \cdot H_2O$ and $pipzSeO_4 \cdot H_2O$ in water. The solution was concentrated on vacuum evaporator; the white crystals obtained were collected under vacuum and recrystallized from water. The composition corresponded to the calculated values (found 34.18% Se, 2.93% Li, 6.11% N, 10.62% C, and 15.95% H_2O; calculated 34.63% Se, 3.04% Li, 6.14% N, 10.52% C, and 15.79% H_2O). In the same way, dilithium N,N'-

Table 3
Bond lengths (Å) and angles (deg) of $Li_2pipz(SeO_4)_2 \cdot 4H_2O$

Se(1)–O(1)	1.633(2)	N(2)–C(1)–C(3)^i	110.1(2)
Se(1)–O(2)	1.635(2)	N(2)–C(1)–H(11)	108(2)
Se(1)–O(4)	1.637(2)	C(3)^i–C(1)–H(11)	112(2)
Se(1)–O(3)	1.638(2)	N(2)–C(1)–H(12)	107(2)
Se(1)–Li3.	171(5)	C(3)^i–C(1)–H(12)	113(2)
O(3)–L^i	1.932(5)	H(11)–C(1)–H(12)	106(3)
O(4)–Li	1.955(5)	C(3)–N(2)–C(1)	111.4(2)
C(1)–N(2)	1.487(4)	C(3)–N(2)–H(21)	107(2)
C(1)–C(3)^i	1.506(4)	C(1)–N(2)–H(21)	110(2)
C(1)–H(11)	0.91(4)	C(3)–N(2)–H(22)	107(3)
C(1)–H(12)	1.03(4)	C(1)–N(2)–H(22)	112(3)
N(2)–C(3)	1.486(4)	H(21)–N(2)–H(22)	110(4)
N(2)–H(21)	0.88(4)	N(2)–C(3)–C(1)^i	109.6(2)
N(2)–H(22)	0.73(4)	N(2)–C(3)–H(31)	107(2)
C(3)–C(1)^i	1.506(4)	C(1)^i–C(3)–H(32)	110(2)
C(3)–H(31)	0.87(4)	H(31)–C(3)–H(32)	111(3)
C(3)–H(32)	0.98(4)	O(6)–Li–O(3)^{ii}	115.9(3)
Li–O(6)	1.914(5)	O(6)–Li–O(5)	109.0(2)
Li–O(3)^{ii}	1.932(5)	O(3)^{ii}–Li–O(5)	103.9(2)
Li–O(5)	1.939(5)	O(6)–Li–O(4)	116.7(3)
Li–H(62)	2.28(5)	O(3)^i–Li–O(4)	105.2(2)
O(5)–H(51)	0.69(5)	O(5)–Li–O(4)	104.9(2)
O(5)–H(52)	0.79(4)	O(6)–Li–Se(1)	104.8(2)
O(6)–H(61)	0.80(5)	O(3)^{ii}–Li–Se(1)	92.8(2)
O(6)–H(62)	0.56(5)	O(5)–Li–Se(1)	130.0(2)
O(1)–Se(1)–O(2)	111.3(1)	O(4)–Li–Se(1)	25.44(9)
O(1)–Se(1)–O(4)	110.2(1)	O(6)–Li–H(62)	12(1)
O(2)–Se(1)–O(4)	109.2(1)	O(3)^{ii}–Li–H(62)	105(1)
O(1)–Se(1)–O(3)	107.3(1)	O(5)–Li–H(62)	110(1)
O(2)–Se(1)–O(3)	109.6(1)	O(4)–Li–H(62)	126(2)
O(4)–Se(1)–O(3)	109.3(1)	Se(1)–Li–H(62)	110(1)
O(1)–Se(1)–Li	114.6(1)	Li–O(5)–H(51)	138(4)
O(2)–Se(1)–Li	127.8(1)	Li–O(5)–H(52)	115(3)
O(4)–Se(1)–Li	30.7(1)	H(51)–O(5)–H(52)	106(5)
O(3)–Se(1)–Li	79.2(1)	Li–O(6)–H(61)	123(3)
Se(1)–O(3)–L^i	132.9(2)	Li–O(6)–H(62)	125(6)
Se(1)–O(4)–Li	123.7(2)	H(61)–O(6)–H(62)	104(6)

Hydrogen bonds

Donor–H	H···Acceptor	Donor···Acceptor	Donor–H···Acceptor
N(2)–H(21)	H(21)···O(3)	N(2)···O(3)	N(2)–H(21)···O(3)
0.88(4)	1.87(4)	2.748(3)	177(3)
N(2)–H(22)^{ii}	H(22)···O(2)^{iii}	N(2)···O(2)^{iii}	N(2)–H(22)···O(2)^{iii}
0.73(4)	2.02(4)	2.734(4)	166(4)
O(5)–H(51)	H(51)···O(4)^{iv}	O(5)···O(4)^{iv}	O(5)–H(51)···O(4)^{iv}
0.69(5)	2.09(6)	2.782(3)	173(6)
O(5)–H(52)	H(52)···O(1)^{v}	O(5)···O(1)^{v}	O(5)–H(52)···O(1)^{v}
0.79(4)	1.96(4)	2.750(3)	176(4)
O(6)–H(61)	H(61)···O(1)^{vi}	O(6)···O(1)^{vi}	O(6)–H(61)···O(1)^{vi}
0.80(5)	1.96(5)	2.763(3)	176(5)
O(6)–H(62)	H(62)···O(2)^{vii}	O(6)···O(2)^{vii}	O(6)–H(62)···O(2)^{vii}
0.56(5)	2.35(5)	2.832(4)	147(7)

Note: Equivalent positions (i) $-x+2, -y, -z$; (ii) $-x+1, -y-1, -z$; (iii) $-x+2, -y, -z+1$; (iv) $-x, -y-1, -z$; (v) $x-1, y-1, z-1$; (vi) $-x+1, -y, -z$; (vii) $x, y, z-1$.

dimethylpiperazinium(2+) selenate tetrahydrate was prepared without studying the corresponding solubility diagram. The composition of the substance correspond to the calculated values (found 33.60% Se, 2.76% Li, 5.48% N, 14.95% C, and 14.69% H_2O; calculated 32.36% Se, 2.84% Li, 5.74% N, 14.77% C, and 14.76% H_2O).

The deuterated compounds $(Li^+)_2(CH_2)_4(ND_2^+)_2$ $(SeO_4^{-2})_2 \cdot 4D_2O$ and $(Li^+)_2(CH_2)_4(ND^+CH_3)_2(SeO_4^{-2})_2 \cdot 4D_2O$ were prepared by repeated recrystallization of natural $Li_2pipz(SeO_4)_2 \cdot 4H_2O$ and $Li_2Me_2pipz(SeO_4)_2 \cdot 4H_2O$, respectively, from D_2O (99%) in a desiccator over KOH.

3.2. Crystal structure of dilithium piperazinium(2+) selenate tetrahydrate

The resulting fractional coordinates with temperature factors U_{eq} are given in Table 2, and selected bond lengths and angles are given in Table 3. The atom numbering can be seen in Fig. 2 and the packing scheme is depicted in Fig. 3. The crystal structure of dilithium piperazinium(2+) selenate tetrahydrate consists of piperazinium(2+) cations and eight member rings formed with two SeO_4 tetrahedra and two LiO_4 tetrahedra connected through tops. The two remaining oxygens on each Li atom come from water molecules. There is a center of symmetry in the middle of this ring. The piperazinium(2+) cations adopt a chair conformation and are arranged roughly plane-parallel above one another. Quite regular tetrahedral SeO_4^{2-} anions exhibit an Se–O bonding distances in the range from 1.633 to 1.638 Å and angles O–Se–O in the range from 109.2° to 111.3° (see Table 3). LiO_4 tetrahedra are slightly deformed with Li–O distances from 1.914 to 1.955 Å and angles O–Li–O in the range 103.9–116.7°. As visible from Table 3, the two water molecules on each Li atom

display different Li–O distances. Both structure units are interconnected by hydrogen bonds of N–H⋯O and O–H⋯O type.

3.3. Crystal structure of dilithium N,N′-dimethylpiperazinium(2+) selenate tetrahydrate

The resulting fractional coordinates with temperature factors U_{eq} are given in Table 4, and selected bond lengths and angles are given in Table 5. The atom numbering can be seen in Fig. 4 and the packing scheme is depicted in Fig. 5. The structure is very similar to structure of $Li_2pipz(SeO_4)_2 \cdot 4H_2O$. It also consists of N,N′-dimethylpiperazinium(2+) cations and eight membered rings formed with two SeO_4 tetrahedra and two LiO_4 tetrahedra connected through tops. The remaining two oxygens on each Li atom are from water molecules. The structure is also centrosymmetric with center of symmetry in the center of eight member ring mentioned above. But the compound crystallize in monoclinic space group $P2_1/c$ with $Z=2$ (the first compound crystallize in triclinic space group $P\bar{1}$ with $Z=1$). The N,N′-dimethylpiperazinium(2+) cations adopt a chair conformation and lie approximately perpendicularly one to another. The slightly deformed tetrahedral SeO_4^{2-} anions exhibit an Se–O bonding distances in the range from 1.624 to 1.642 Å (see Table 5). Different bond lengths Se–O are due to different hydrogen acceptor behavior: longer bonds are due to the fact that the O-atoms act twice as H-acceptor since in the shorter bonds oxygen acts just once H-acceptor [11]. SeO_4 tetrahedral angles lie in the range from 108.8° to 110.0°, which represents quite regular geometry (see Table 5). LiO_4 tetrahedra are deformed with Li–O distances from 1.916 to 1.989 Å and angles O–Li–O in the range 96.8 – 119.0°. As evident from Table 5, the two water molecules on each Li atom display different Li–O distances. Both
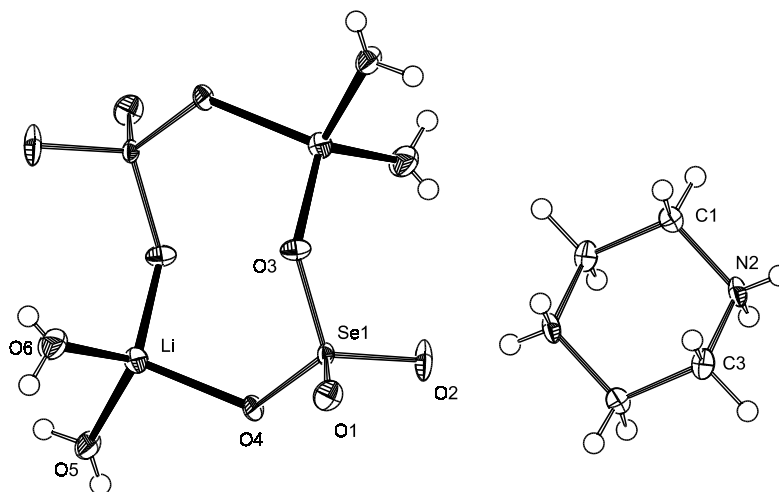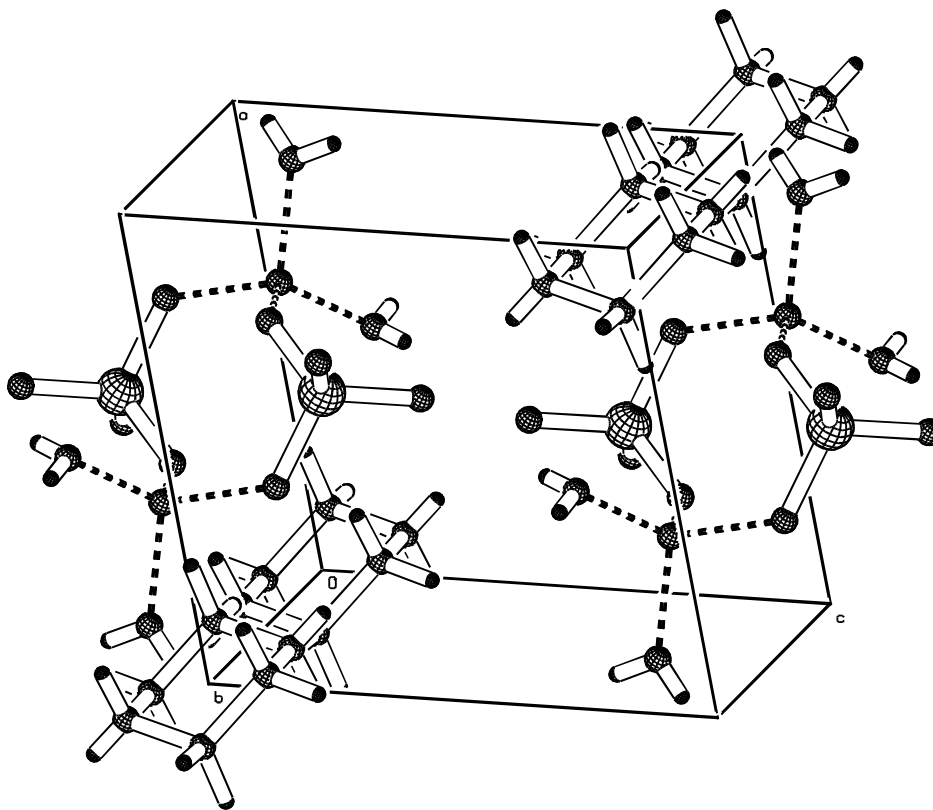

Fig. 2. Atom numbering of $Li_2pipz(SeO_4)_2 \cdot 4H_2O$.

Fig. 3. Packing scheme of $Li_2pipz(SeO_4)_2 \cdot 4H_2O$. Dashed lines represent coordination bonds in LiO_4 polyhedra.

Table 4
Fractional atomic coordinates (for non-H atoms $\times 10^4$, for H atoms $\times 10^3$) and equivalent or isotropic displacement factors of $Li_2Me_2pipz(SeO_4)_2 \cdot 4H_2O$

	x	y	z	U_{eq} (Å)
Se(1)	3174(1)	353(1)	8277(1)	10(1)
O(1)	1836(3)	1730(2)	7848(2)	22(1)
O(2)	3658(3)	−797(3)	7319(2)	20(1)
O(3)	2125(3)	−617(2)	9166(2)	15(1)
O(4)	5035(3)	1090(2)	8777(2)	19(1)
O(5)	−1509(3)	−1320(2)	8841(2)	18(1)
O(6)	−1296(3)	2382(2)	8902(2)	17(1)
C(1)	−3361(4)	5896(3)	10002(2)	14(1)
N(2)	−3770(3)	4928(3)	10918(2)	13(1)
C(3)	−4915(4)	3593(3)	10566(2)	15(1)
C(4)	−2068(4)	4412(4)	11462(3)	19(1)
Li	7395(7)	517(5)	9332(4)	16(1)
H(11)	−266(4)	534(3)	957(2)	2(7)
H(12)	−261(4)	673(4)	1025(2)	23(8)
H(21)	−445(5)	542(3)	1138(3)	8(8)
H(31)	−528(4)	304(4)	1120(2)	16(7)
H(32)	−406(5)	294(4)	1010(3)	25(8)
H(41)	−157(5)	527(4)	1176(3)	16(9)
H(42)	−228(4)	395(4)	1198(3)	14(8)
H(43)	−154(4)	377(4)	1102(3)	24(9)
H(51)	−50(5)	−120(4)	890(3)	21(10)
H(52)	−166(5)	−187(7)	836(3)	45(15)
H(61)	−53(6)	220(5)	866(3)	26(12)
H(62)	−196(5)	287(6)	847(3)	39(12)

$U_{eq} = 1/3 \sum_i \sum_j U_{ij} a_i^* a_j^* \mathbf{a}_i \mathbf{a}_j.$

structure units are interconnected by hydrogen bonds of $N–H \cdots O$ and $O–H \cdots O$ type.

3.4. Analysis of the vibrational spectra

The numbers of normal modes of the $Li_2pipz(SeO_4)_2 \cdot 4H_2O$ and $Li_2Me_2pipz(SeO_4)_2 \cdot 4H_2O$ crystals were determined by nuclear site group analysis [12].

The $Li_2pipz(SeO_4)_2 \cdot 4H_2O$ crystals belong in the $P\bar{1}$ (C_i^1) space group with 21 atoms per asymmetric unit $(Z=1)$. All the atoms occupy twofold positions $i(C_1)$. Five types of species present in the unit cell, piperazinium(2+) cation SeO_4^{2-} anion, LiO_4 tetrahedra and two water molecules, occupying one fold positions $a(C_i)$ (piperazinium cation) and twofold positions $i(C_1)$ (the rest of species), were considered in more detailed calculations of the internal and external modes. The results are representations $27A_g(RA) + 24A_u(IR)$ for external modes (excluding acoustic modes), and $36A_g(RA) + 36A_u(IR)$ for internal modes.

The $Li_2Me_2pipz(SeO_4)_2 \cdot 4H_2O$ crystals belong in the $P2_1/c$ (C_{2h}^5) space group with 24 atoms per asymmetric unit $(Z=2)$. All the atoms occupy fourfold positions $e(C_1)$. Five types of species present in the unit cell, dimethylipiperazinium(2+) cation, SeO_4^{2-} anion, LiO_4 tetrahedra and two water molecules, occupying twofold positions $d(C_i)$ (dimethyli-piperazinium cation) and

Table 5
Bond lengths (Å) and angles (deg) of $Li_2Me_2pipz(SeO_4)_2 \cdot 4H_2O$

Se(1)–O(4)	1.6236(18)	Li^{ii}–O(5)–H(51)	106(3)
Se(1)–O(3)	1.640(2)	Li^{ii}–O(5)–H(52)	136(3)
Se(1)–O(1)	1.6416(19)	H(51)–O(5)–H(52)	106(4)
Se(1)–O(2)	1.642(2)	Li^{ii}–O(6)–H(61)	111(4)
O(3)–Li^{i}	1.953(5)	Li^{ii}–O(6)–H(62)	109(3)
O(4)–Li	1.916(5)	H(61)–O(6)–H(62)	107(4)
O(5)–Li^{ii}	1.921(5)	N(2)–C(1)–C(3)^{iii}	111.3(2)
O(5)–H(51)	0.75(4)	N(2)–C(1)–H(11)	108(2)
O(5)–H(52)	0.79(5)	C(3)^{iii}–C(1)–H(11)	110(2)
O(6)–Li^{ii}	1.989(5)	N(2)–C(1)–H(12)	108(2)
O(6)–H(61)	0.68(4)	C(3)^{iii}–C(1)–H(12)	113(2)
O(6)–H(62)	0.84(5)	H(11)–C(1)–H(12)	106(2)
C(1)–N(2)	1.492(3)	C(4)–N(2)–C(1)	111.0(2)
C(1)–C(3)^{iii}	1.506(4)	C(4)–N(2)–C(3)	110.8(2)
C(1)–H(11)	0.91(3)	C(1)–N(2)–C(3)	109.5(2)
C(1)–H(12)	0.97(4)	C(4)–N(2)–H(21)	108(2)
N(2)–C(4)	1.481(4)	C(1)–N(2)–H(21)	112(2)
N(2)–C(3)	1.504(4)	C(3)–N(2)–H(21)	105(2)
N(2)–H(21)	0.91(3)	N(2)–C(3)–C(1)^{iii}	111.3(2)
C(3)–C(1)^{iii}	1.506(4)	N(2)–C(3)–H(31)	108(2)
C(3)–H(31)	1.00(3)	C(1)^{iii}–C(3)–H(31)	107(2)
C(3)–H(32)	1.05(4)	N(2)–C(3)–H(32)	105(2)
C(4)–H(41)	0.92(4)	C(1)^{iii}–C(3)–H(32)	113(2)
C(4)–H(42)	0.80(3)	H(31)–C(3)–H(32)	113(3)
C(4)–H(43)	0.90(4)	N(2)–C(4)–H(41)	105(2)
Li–O(5)^{iv}	1.921(5)	N(2)–C(4)–H(42)	111(2)
Li–O(3)^{i}	1.953(5)	H(41)–C(4)–H(42)	99(3)
Li–O(6)^{iv}	1.989(5)	N(2)–C(4)–H(43)	106(2)
O(4)–Se(1)–O(3)	109.9(1)	H(41)–C(4)–H(43)	127(3)
O(4)–Se(1)–O(1)	108.9(1)	H(42)–C(4)–H(43)	108(3)
O(3)–Se(1)–O(1)	109.1(1)	O(4)–Li–O(5)^{iv}	118.8(3)
O(4)–Se(1)–O(2)	110.0(1)	O(4)–Li–O(3)^{i}	119.0(3)
O(3)–Se(1)–O(2)	108.8(1)	O(5)^{iv}–Li–O(3)^{i}	107.5(2)
O(1)–Se(1)–O(2)	110.2(1)	O(4)–Li–O(6)^{iv}	96.8(2)
Se(1)–O(3)–Li^{i}	126.4(2)	O(5)^{iv}–Li–O(6)^{iv}	113.0(3)
Se(1)–O(4)–Li	141.1(2)	O(3)^{i}–Li–O(6)^{iv}	99.5(2)

Hydrogen bonds

Donor–H	H···Acceptor	Donor···Acceptor	Donor–H···Acceptor
N(2)–H(21)	H(21)···O(2)^{v}	N(2)···O(2)^{v}	N(2)–H(21)···O(2)^{v}
0.91(3)	1.89(4)	2.763(3)	159(3)
O(5)–H(51)	H(51)···O(3)	O(5)···O(3)	O(5)–H(51)···O(3)
0.75(4)	2.01(4)	2.755(3)	172(4)
O(5)–H(52)	H(52)···O(1)^{vi}	O(5)···O(1)^{vi}	O(5)–H(52)···O(1)^{vi}
0.79(5)	1.98(5)	2.771(3)	175(4)
O(6)–H(61)	H(61)···O(1)	O(6)···O(1)	O(6)–H(61)···O(1)
0.68(4)	2.09(4)	2.769(3)	177(5)
O(6)–H(62)	H(62)···O(2)^{vii}	O(6)···O(2)^{vii}	O(6)–H(62)···O(2)^{vii}
0.84(5)	1.97(5)	2.799(3)	170(4)

Note: Equivalent positions (i) $-x+1, -y, -z+2$; (ii) $x-1, y, z$; (iii) $-x-1, -y+1, -z+2$; (iv) $x+1, y, z$; (v) $x-1, y+\frac{1}{2}, z+\frac{1}{2}$; (vi) $-x, y-\frac{1}{2}, -z+\frac{3}{2}$; (vii) $-x, y+\frac{1}{2}, -z+\frac{3}{2}$.

fourfold positions $e(C_1)$ (the rest of species), were considered in more detailed calculations of the internal and external modes. The results are representations $27A_g(RA) + 26A_u(IR) + 27B_g(RA) + 25B_u(IR)$ for external modes (excluding acoustic modes), and $45A_g(RA) + 45A_u(IR) + 45B_g(RA) + 45B_u(IR)$ for internal modes.

Standard correlation method [13] was used for detailed study of the expected vibrational features of the SeO_4^{2-} groups in both the structures. The results obtained are presented in Tables 6 and 8.

3.5. Vibrational spectra

The vibrational spectra of $Li_2pipz(SeO_4)_2 \cdot 4H_2O$ and $Li_2Me_2pipz(SeO_4)_2 \cdot 4H_2O$ are depicted in Figs. 6 and 7, the wavenumbers of the observed bands are given in
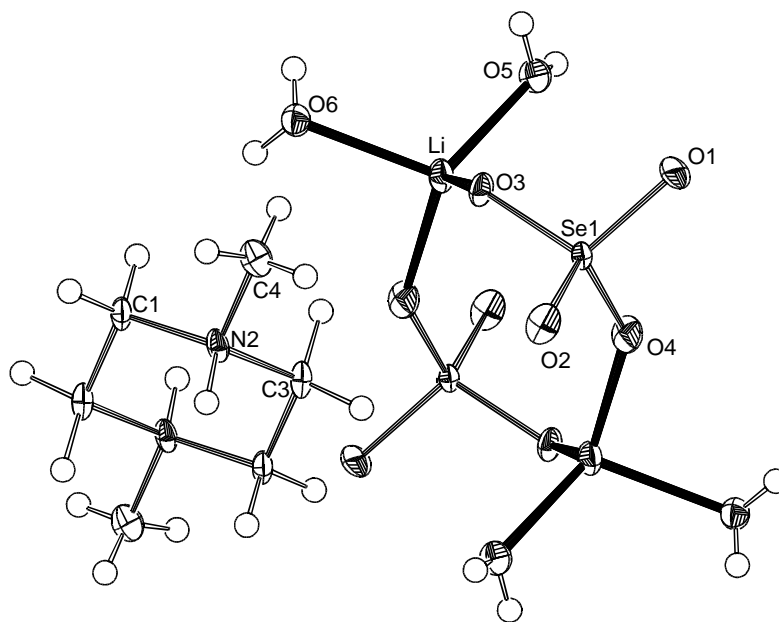
Fig. 4. Atom numbering of $Li_2Me_2pipz(SeO_4)_2 \cdot 4H_2O$.
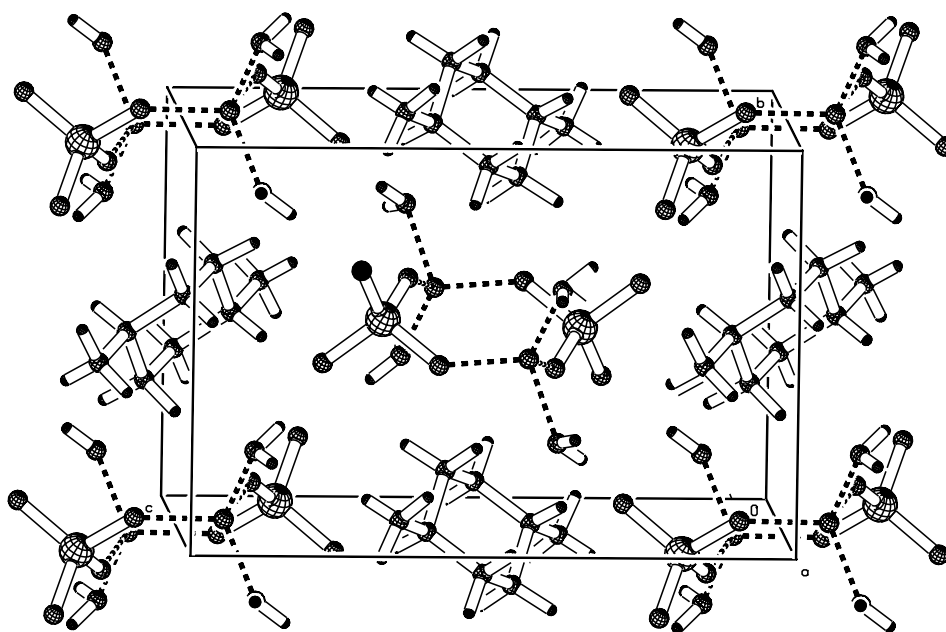
Fig. 5. Packing scheme of $Li_2Me_2pipz(SeO_4)_2 \cdot 4H_2O$. Dashed lines represent coordination bonds in LiO_4 polyhedra.

Table 6
Correlation analysis of SeO_4^{2-} internal modes in $Li_2pipz(SeO_4)_2 \cdot 4H_2O$ crystal

Free ion modes	Degrees of freedom	Free ion symmetry T_d	Site symmetry C_1	Factor group symmetry C_i	Vibrational modes	Activity	
						IR	Raman
v_1	2	A_1		A_g	$v_1, 2v, 3v_3, 3v_4$		All α
v_2	2	E					
v_3	2	F_2	A				
v_4	2	F_2		A_u	$v_1, 2v_2, 3v_3, 3v_4$	x, y, z	

Table 7
FTIR and FT Raman spectra $Li_2pipz(SeO_4)_2 \cdot 4H_2O$

Assignment	IR	Raman (intensity)	Assignment	IR	Raman (intensity)
νO–H$\cdots$O	3535 m		δCNH, δNCH, δCCH	1326 w	1316(9)
	3495 m		δNCH, δCCH	1219 w	1213(1)
	3350 sb	3350(1)		1160 wb	1165(2)
	3290 sb	3280(1)	ωCH$_2$, ρNH$_2^+$	1087 m	1063(6)
νCH$_2$	3044 m	3045(14)	ωCH$_2$		1045(8)
	3014 m	3014(11)	ρNH$_2^+$	1011 m	
	2995 sh	2991(13)	γN-H...O	975 w	
	2969 m	2972(29)	?		913(3)
νN–H$\cdots$O	2913 m	2919(4)	ν_3 (SeO$_4^{2-}$)	887 s	873(33)
		2880(3)		877 s	
	2856 m	2853(2)		868 s	
	2809 m	2815(3)	ν_1 (SeO$_4^{2-}$)		852(100)
	2759 m	2770(4)	νCN, δCNC, δNCH		828(9)
	2733 m				818(11)
	2685 m	2686(2)	ρH$_2$O	700 mb	
	2629 m	2637(2)	δCNH, δCCH, δNCC	595 m	
	2589 m	2587(1)	νLi–O	490 m	
	2514 m	2505(2)	δNCC, δCCH, δCNC		467(9)
	2480 m				446(8)
?	2223 w		ν_4 (SeO$_4^{2-}$)		430(6)
	2174 w			420 m	416(6)
	1988 w			401 m	
	1940 w				388(5)
	1886 w		ν_2 (SeO$_4^{2-}$)		359(15)
δH$_2$O	1682 m				317(10)
	1656 m		External modes		242(1)
δH$_2$O, δNH$_2^+$	1627 m	1632(1)			180(1)
δCH$_2$	1470 m	1467(4)			163(1)
	1462 m				121(10)
	1451 m	1444(15)			103(6)
twi CH$_2$		1411(3)			
	1386 w				

Note. Abbreviations—s, strong; m, medium; w, weak; b, broad; sh, shoulder; ν, stretching; δ deformation or in-plane bending; γ, out-of-plane bending; twi, twisting.

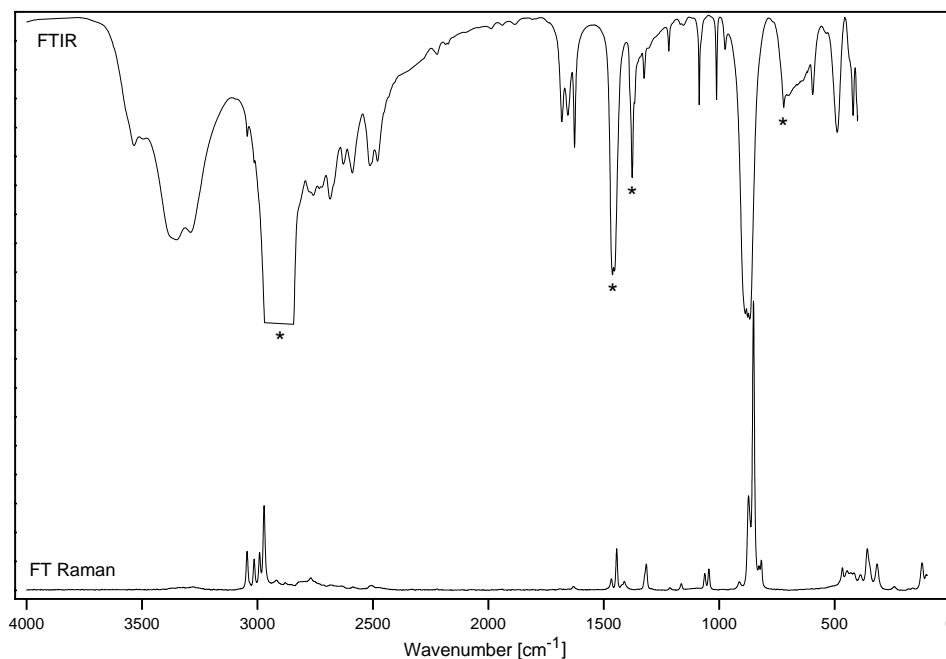Fig. 6. FTIR (nujol mull) and FT Raman spectra of $Li_2pipz(SeO_4)_2 \cdot 4H_2O$. Nujol bands are indicated by asterisk.
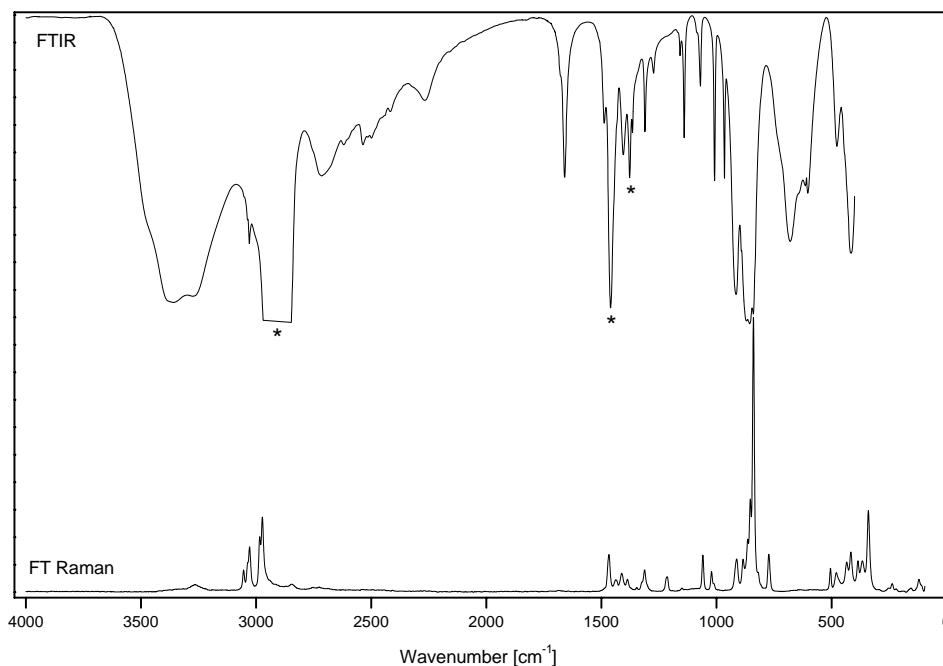
Fig. 7. FTIR (nujol mull) and FT Raman spectra of $Li_2Me_2pipz(SeO_4)_2 \cdot 4H_2O$. Nujol bands are indicated by asterisk.

Table 8
Correlation analysis of SeO_4^{2-} internal modes in $Li_2Me_2pipz(SeO_4)_2 \cdot 4H_2O$ crystal

Free ion modes	Degrees of freedom	Free ion symmetry T_d	Site symmetry C_1	Factor group symmetry C_{2h}	Vibrational modes	Activity	
						IR	Raman
v_1	4	A_1		A_g	$v_1, 2v_2, 3v_3, 3v_4$		$\alpha_{xx}, \alpha_{yy}, \alpha_{zz}, \alpha_{xy}$
v_2	4	E	A	A_u	$v_1, 2v_2, 3v_3, 3v_4$	z	
v_3	4	F_2		B_g	$v_1, 2v_2, 3v_3, 3v_4$		α_{xz}, α_{yz}
v_4	4	F_2		B_u	$v_1, 2v_2, 3v_3, 3v_4$	x, y	

Tables 7 and 9, respectively. Detailed interpretation of the spectra is based on previous study of piperazine [14–16], N,N'-dimethylpiperazine [17–19] and selenate anions [20] and is also consistent with our earlier results published for similar compounds of piperazinium selenates family [1]. The IR spectra of N,O-deuterated compounds were also recorded in order to confirm presented interpretation.

Broad, intense bands in the IR spectra of both compounds in the 3500–3200 cm^{-1} region correspond to stretching O–H vibrations of water molecules connected by weak O–H···O hydrogen bonds to anions. Manifestations of cation–anion (N–H···O) hydrogen bonds are very broad medium-intensity bands with centre at about 2700 cm^{-1}. The presence of sub-bands of the vO–H···O and especially vN–H···O vibrations is probably a result of interactions with overtones and combination bands. According to Lautie et al. [21] and Novak [22] the positions of vO–H···O and vN–H···O vibrational bands correspond well to H-bonds found in the

crystal structures of $Li_2pipz(SeO_4)_2 \cdot 4H_2O$ and Li_2Me_2 $pipz(SeO_4)_2 \cdot 4H_2O$ with lengths of 2.75–2.83 Å (O–H···O) and 2.73–2.76 Å (N–H···O). The weak band at 975 cm^{-1} (the case of $Li_2pipz(SeO_4)_2 \cdot 4H_2O$) and weak to medium-intesity bands in the 1070–965 cm^{-1} region (the case of $Li_2Me_2pipz(SeO_4)_2 \cdot 4H_2O$) can be assigned to manifestations of out-of-plane N–H···O bending vibrations in the IR spectra. The similar bands of γO–H···O vibrations are evidently overlapped by the stretching vibrations of the selenate anions. Corresponding shifts of all the bands of the stretching and out-of-plane bending vibrations were observed in the spectra of the N,O-deuterated compounds.

The presence of crystal water molecules is indicated by the bands of δH_2O and ρH_2O vibrations at 1680–1630 cm^{-1} and 700–615 cm^{-1} regions, respectively. The bands of H_2O deformation vibrations are partially overlapping with δNH_2^+ bands in the IR spectrum of $Li_2pipz(SeO_4)_2 \cdot 4H_2O$. All the bands discussed are sensitive to deuteration, as expected.

Table 9
FTIR and FT Raman spectra $Li_2Me_2pipz(SeO_4)_2 \cdot 4H_2O$

Assignment	IR	Raman (intensity)	Assignment	IR	Raman (intensity)
νO–H···O	3360 sb		νCC, νCN, δNCH	1159 w	1151(1)
	3270 sb	3265(3)		1141 m	
νCH$_2$, νCH$_3$		3055(8)		1087 sh	
		3037(10)	γN–H···O	1070 w	1060(13)
	3029 m	3029(16)	δNCH, δCCH, νCN		1022(7)
	3007 m		γN–H···O, δNCH, δCCH, νCN	1009 m	1012(3)
		2985(20)	γN–H···O	965 m	
		2973(26)	ν_3(SeO$_4^{2-}$)	916 s	912(12)
	2950 m				885(12)
νN–H···O	2885 m			870 s	865(19)
		2846(3)		856 s	854(34)
	2820 m		ν_1(SeO$_4^{2-}$)	840 s	840(100)
	2710 m		?		820(7)
	2620 w		νCN		774(14)
	2536 m		ρH$_2$O	681 mb	
	2499 m			642 sh	
	2417 w			614 mb	
	2268 m		?	604 m	
δH$_2$O	1660 m		δCNC, δNCC		505(9)
δNH$^+$	1488 m		νLi–O	477 m	480(6)
δ_{as}CH$_3$, δCH$_2$	1460 s	1467(14)	δNCC, δCCH, δCNC		435(10)
	1431 m	1439(4)	ν_4(SeO$_4^{2-}$)	415 m	417(14)
δ_sCH$_3$, twi CH$_2$	1405 m	1412(7)			386(11)
	1380 sh	1388(5)	ν_2(SeO$_4^{2-}$)		367(11)
	1365 m				341(29)
δNCH, δCCH		1347(2)	External modes		254(1)
		1325(3)			237(3)
	1311 m	1313(8)			221(1)
	1274 w				155(2)
δCCH, δNCH		1218(5)			121(6)
		1214(5)			110(4)

Note: subscripts—s, symmetric; as, antisymmetric.

A number of sharp bands which occur in the 3055–2950 cm^{-1} interval (especially in the Raman spectra) are characteristic for the stretching vibrations of the CH$_2$ and CH$_3$ groups. Manifestations of deformation vibrations of these groups are localized in the 1470–1365 cm^{-1} region.

Bands of the NH$_2^+$ and NH$^+$ groups deformation vibrations (1630–1490 cm^{-1} region) together with bands of ρNH$_2^+$ vibrations at 1090–1010 cm^{-1} (the case of Li$_2$pipz(SeO$_4$)$_2 \cdot$4H$_2$O) clearly indicate the presence of piperazinium(2+) and dimethylpiperazinium(2+) cations in the crystal structures. As expected, these bands are sensitive to deuteration. Vibrational manifestations of the whole cations were observed below 1350 cm^{-1} in the spectra.

Observed level of factor group splitting of selenate anions internal vibrations is slightly lower than correlation analysis results (see Tables 6 and 8). This fact could be explained by small inter-ion interaction in the unit cell and also in terms of the fact that all the measurements were carried out on polycrystalline samples at the temperature of 298 K. Anyway, lower factor group symmetry of selenates in the crystal

structure of Li$_2$Me$_2$pipz(SeO$_4$)$_2 \cdot$4H$_2$O results in the presence of ν_1 vibration (840 cm^{-1}) in the IR spectrum together with higher splitting of ν_3 vibration (900–860 cm^{-1} region). Quite surprising is the fact that observed splitting of triple degenerate vibration ν_4 is even lower than in the spectra of Li$_2$pipz(SeO$_4$)$_2 \cdot$4H$_2$O.

The presence of LiO$_4$ moieties in both the crystal structures is indicated by the medium-intensity bands (IR spectra) of the stretching Li–O vibrations at ca. 480–490 cm^{-1}.

Manifestations of external modes were recorded in the Raman spectra of both compounds in the region under 250 cm^{-1}.

3.6. Thermal behavior

The loss of the moisture ends at 373 K ($\sim$4.5%) and decomposition begins at nearly the same temperature for Li$_2$pipz(SeO$_4$)$_2 \cdot$4H$_2$O. All the water is liberated in one wave accompanied with deep endo effect in the range 373–408 K. Anhydrous salt is stable up to 533 K, when total decomposition begins accompanied with a huge exo effect with maximum at 648 K. The total loss

after this temperature represents more than 98% of the original sample.

$Li_2Me_2pipz(SeO_4)_2 \cdot 4H_2O$ is stable up to 378 K, when the decomposition begins. In spite of the fact, that in the crystal structure exist two pairs of water molecules with the same environment, the loss of water is divided into two waves corresponding approximately to three molecules and one molecule of water, respectively. Total loss of water corresponds well to four molecules and ends at 453 K, when total decomposition begins. The loss of water is accompanied with two well resolved endo effects, the total decomposition with a huge exo effect.

Study of both compounds by the DCS method was carried out in the temperature interval 95–343 K no effect that would correspond to a phase transition was observed. As the point groups of both the test compounds do not correspond to any of the 10 polar crystallographic classes and a phase transition to a polar group has not been found, these two compounds cannot exhibit ferroelectric properties in the temperature interval 95–343 K. Similarly, no phase transition was found that would lead at elevated temperature to the formation of crystallographic phases with fast proton conductivity.

Acknowledgments

References

[1] D. Havlíček, J. Plocek, I. Němec, R. Gyepes, Z. Mička, J. Solid State Chem. 150 (2000) 305.
[2] T. Noto, H. Sawada, Y. Sato, N. Fukuda, K. Kotera, Yakuguku Kenkyu 30 (1958) 712.
[3] D.B. Rollins, H.N. Calderwood, J. Am. Chem. Soc. 60 (1938) 2751.
[4] Th. Dippel, N. Hainovksy, K.D. Kreuer, W. Münch, V. Maier, Ferroelectrics 167 (1995) 59.
[5] F.A.H. Schreinemakers, Z. Phys. Chem. 11 (1893) 75.
[6] V. Petříček, M. Dušek, Crystallographic Computing System, Institute of Physics, Czech Academy of Science, Praha, 1998.
[7] A.L. Spek, PLATON, A Multipurpose Crystallographic Tool, Utrecht University, Utrecht, 2000.
[8] A. Altomare, M.C. Burla, M. Camalli, G. Cascarano, L. Giacovazzo, A. Gualigardi, G. Poliadori, J. Appl. Crystallogr. 27 (1994) 435.
[9] G.M. Sheldrick, SHELX 97, University of Göttingen, Göttingen, 1997.
[10] B. Blanka, P. Hudec, P. Mošna, J. Toužín, Collection Czech. Chem. Commun. 28 (1963) 3434.
[11] E. Kemnitz, S.J. Troyanov, in: M. Hargiatti, I. Hargiatti (Eds.), Advances in Molecular Structure Research, Vol. 4, JAI Press, New York, 1998, pp. 79–113.
[12] D.L. Rousseau, R.P. Bauman, S.P.S. Porto, J. Raman Spectrosc. 10 (1981) 253.
[13] W.G. Fateley, N.T. McDevit, F.F. Bentley, Appl. Spectrosc. 25 (1971) 155.
[14] S.M. Kim, V.I. Pesterev, Kh.Kh. Muldagaliev, V.Z. Gabdrakipov, O.V. Agashkin, Zh. Fiz. Khim. 53 (3) (1979) 557.
[15] Kh.Kh. Muldagaliev, O.V. Agashkin, Izv. Akad. Nauk Kaz. SSR Ser. Khim. (6) (1980) 42.
[16] P.J. Hendra, D.B. Powell, Spectrochim. Acta 18 (1962) 299.
[17] N.N. Rubanyuk, S.M. Kim, Kh.Kh. Muldagaliev, O.V. Agashkin, Izv. Akad. Nauk Kaz. SSR Ser. Khim. (5) (1986) 38.
[18] S.M. Kim, Kh.Kh. Muldagaliev, O.V. Agashkin, Izv. Akad. Nauk Kaz. SSR Ser. Khim. (4) (1989) 14.
[19] K. Fukushima, Bull. Chem. Soc. Jpn. 52 (10) (1979) 2871.
[20] K. Nakamoto, In: Infrared and Raman Spectra of Inorganic and Coordination Compounds, 4th Edition, Wiley, New York, 1986, p. 138.
[21] A. Lautie, F. Froment, A. Novak, Spectrosc. Lett. 9 (5) (1976) 289.
[22] A. Novak, Struct. Bonding 18 (1974) 177.